Multiplexing efficiency of MIMO antennas in arbitrary propagation scenarios

Tian, Ruiyuan; Lau, Buon Kiong; Ying, Zhinong

Published in:
6th European Conference on Antennas and Propagation (EUCAP), 2012

DOI:
10.1109/EuCAP.2012.6205897

2012

Document Version:
Peer reviewed version (aka post-print)

R. Tian, B. K. Lau, and Z. Ying, “Multiplexing efficiency of MIMO antennas in arbitrary propagation scenarios,” in *Proc. 6th Europ. Conf. Antennas Propagat. (EuCAP’2012)*, Prague, Czech Republic, Mar. 26-30, 2012.

Multiplexing Efficiency of MIMO Antennas in Arbitrary Propagation Scenarios

Ruiyuan Tian[1], Buon Kiong Lau[1] and Zhinong Ying[2]
[1]Department of Electrical and Information Technology, Lund University, Sweden
[2]Sony Ericsson Mobile Communications AB, Sweden
Email: Buon_Kiong.Lau@eit.lth.se

***Abstract*—Multiplexing efficiency has recently been proposed as a performance metric for characterizing the absolute efficiency of MIMO antennas in a reference channel. In this work, we generalize this metric to account for arbitrary propagation channels, so the impact of the channel can also be studied. Using the extended definition of multiplexing efficiency, the respective roles of effective antenna gain and signal correlation due to non-isotropic incident fields can be clearly identified. A numerical evaluation based on two MIMO terminal prototypes and four different propagation scenarios is performed to demonstrate the effectiveness of the generalized metric. We find that the MIMO antenna with high total antenna efficiency and good pattern diversity offers a robust multiplexing efficiency performance in all the considered propagation scenarios.**

I. Introduction

With the recent adoption of MIMO technology in major wireless communication standards, performance characterization of multi-antennas in mobile terminals is a subject of current interest. The challenge in characterizing multi-antenna performance lies in that many parameters are important in determining the overall performance, including antenna efficiency, correlation, branch power imbalance, etc. In a MIMO system, the performance of different multi-antennas is usually evaluated and compared in terms of channel capacity. However, the capacity metric does not adequately isolate the impact of different antenna impairments on the performance of MIMO systems or give a definitive measure of the absolute efficiency of multi-antennas. Furthermore, channel capacity is an information theoretic metric that is less intuitive to antenna designers, who would benefit more from a power related measure, such as the diversity gain. Since spatial multiplexing is the primary mechanism for increasing the spectral efficiency in MIMO systems, it is important to consider it explicitly in the design of multi-antennas.

For this purpose, a simple and intuitive metric "multiplexing efficiency" is recently proposed in [1]. The multiplexing efficiency metric η_{mux} defines the loss of power efficiency when using a MIMO antenna-under-test (AUT) to achieve the same performance as that of a reference antenna system in the same propagation channel. It can be interpreted as a generalization of the total antenna efficiency concept for single antennas to the case of multi-antennas. For the case of a two-element MIMO antenna, a closed form expression of η_{mux} has been derived for a reference propagation channel with uniform 3D angular power spectrum (APS),

$$\tilde{\eta}_{\mathrm{mux}} = \sqrt{\eta_1 \eta_2 (1 - |r|^2)}, \tag{1}$$

where η_1 and η_2 denote the total efficiency of the two antenna elements, and $|r|$ denotes the magnitude of complex correlation between them. The unique features of the expression are both its simplicity and the valuable insights it offers with respect to the performance impact of non-ideal behaviors of MIMO antennas, *i.e.*, correlation, non-ideal total efficiency and efficiency imbalance. Because of its unique features, multiplexing efficiency is ideal for evaluating the effectiveness of MIMO terminal antennas in realistic user scenarios [2]. A recent study also shows that the performance evaluations with the multiplexing efficiency metric can lead to similar conclusions as those obtained from performing full-scale link-level simulation [3], which further confirms the effectiveness of the simple metric in giving realistic and meaningful results.

Nevertheless, the discussion of multiplexing efficiency in [1] is confined to the reference propagation scenario of uniform 3D APS. In this paper, we show that the multiplexing efficiency metric can be generalized for evaluating MIMO antennas under propagation scenarios with arbitrary APSs. In Section II, the concept of multiplexing efficiency is revisited and the extension to consider an arbitrary APS using the mean effective gain (MEG) concept is derived. In Section III, the evaluation procedure is formulated. Section IV performs a numerical analysis on two two-element MIMO antenna prototypes. Section V concludes the paper.

II. Multiplexing Efficiency Metric

First, we briefly review the concept of multiplexing efficiency as proposed in [1]. Without any loss of generality, the case of receive antennas is examined. The MIMO channel is given by

$$\mathbf{H} = \mathbf{R}^{1/2} \mathbf{H}_{\mathrm{w}}, \tag{2}$$

where $\mathbf{R}$ denotes the receive correlation matrix, and $\mathbf{H}_{\mathrm{w}}$ denotes an independent and identically distributed (IID) Rayleigh fading channel. In order to characterize the power efficiency of MIMO AUTs with respect to a reference MIMO antenna that achieves the same channel capacity, the multiplexing efficiency is defined as

$$\eta_{\mathrm{mux}} = \frac{P_{\mathrm{T},0}}{P_{\mathrm{T}}}, \tag{3}$$

This work was financially supported by Vetenskapsrådet (Grant no. 2010-468) and VINNOVA (Grant no. 2009-02969).

where $P_{\mathrm{T},0}$ and P_{T} denote the required power for achieving the same capacity performance with the reference antenna and the MIMO AUT, respectively. For high SNRs, η_{mux} is readily obtained as

$$\tilde{\eta}_{\mathrm{mux}} = \lim_{P_{\mathrm{T}}\to\infty} \eta_{\mathrm{mux}} = \frac{P_{\mathrm{T},0}}{P_{\mathrm{T}}} = \frac{\det(\mathbf{R})^{1/M}}{\det(\mathbf{R}_0)^{1/M}}, \tag{4}$$

where $\mathbf{R}_0$ and $\mathbf{R}$ are the receive correlation matrices when using the reference antenna and the MIMO AUT in the same propagation channel, respectively. As discussed in [1], the exact value η_{mux} converges well to the limit $\tilde{\eta}_{\mathrm{mux}}$ at commonly used reference SNR values.

The matrix $\mathbf{R}$ fully describes the effects of the antennas on the channel. In particular, it can be decomposed as

$$\mathbf{R} = \mathbf{\Lambda}^{1/2}\bar{\mathbf{R}}\mathbf{\Lambda}^{1/2}, \tag{5}$$

where the (i,j)-th element of $\bar{\mathbf{R}}$ is the correlation coefficient between the i-th and j-th antennas, and $\mathbf{\Lambda}$ represents a diagonal matrix given by

$$\mathbf{\Lambda} = \mathrm{diag}[\gamma_1, \gamma_2, \cdots, \gamma_M], \tag{6}$$

where γ_i characterizes the gain of the ith antenna, which is simply the total efficiency of the i-th antenna η_i in the case of uniform 3D APS. The correlation coefficient and total gain of the respective reference antenna and MIMO AUT can be calculated using well-known expressions, given the statistical function that characterizes the APS of the incident field at the antennas. In the following, we describe each of these parameters in some detail.

A. Propagation Channel

According to the channel model given in (2), the impact of the propagation channel is fully characterized by the incident field at the antenna system, which can be described by a statistical distribution of the APS as

$$P_{\theta,\phi}(\Omega) = P_{\theta}(\Omega)\widehat{\theta} + P_{\phi}(\Omega)\widehat{\phi}. \tag{7}$$

In this study, two types distributions are considered for the APS. First, as a reference scenario, we consider a completely random environment of uniform distribution, *i.e.*,

$$P_{\mathrm{Uniform}}(\Omega) \propto 1. \tag{8}$$

For the second type, we consider the Gaussian distribution, which is a statistically appealing form for the APS [4], given by

$$P_{\mathrm{Gaussian}}(\theta,\phi) \propto \exp\left[-\left(\frac{(\theta-\theta_0)^2}{2\sigma_\theta^2} + \frac{(\phi-\phi_0)^2}{2\sigma_\phi^2}\right)\right], \tag{9}$$

where the mean incident direction is denoted by (θ_0, ϕ_0) with angular spread $(\sigma_\theta, \sigma_\phi)$. The discussion can easily be extended to the use of a Laplacian distribution, which is identified as a better model of the APS in some scenarios [4].

B. Mean Effective Gain

In order to evaluate the effective gain of an antenna averaged over a given propagation scenario, we adopt the mean effective gain (MEG) metric [5]. The MEG metric G_{e} is defined as the ratio between the mean received power of the antenna and the total mean incident power available to the antenna, *i.e.*,

$$G_{\mathrm{e}} = \int \chi G_{\theta}(\Omega)P_{\theta}(\Omega) + G_{\phi}(\Omega)P_{\phi}(\Omega)\,\mathrm{d}\Omega, \tag{10}$$

where χ denotes the cross-polarization ratio (XPR), and the antenna gain is given by $G_{\theta,\phi}(\Omega) = |E_{\theta,\phi}(\Omega)|^2$. $E_{\theta,\phi}(\Omega)$ represents the complex radiation pattern of the antenna

$$E_{\theta,\phi}(\Omega) = E_{\theta}(\Omega)\widehat{\theta} + E_{\phi}(\Omega)\widehat{\phi}. \tag{11}$$

For ideal isotropic antennas where $G_{\theta,0} = G_{\phi,0}$ is a constant regardless of the direction Ω, the MEG of $G_{\mathrm{e},0} = 1/2$ is always obtained, regardless of the propagation scenario. On the other hand, for the uniform 3D APS scenario, which is given by $\chi = 1$ and $P_{\theta,\phi}(\Omega) = P_{\mathrm{Uniform}}(\Omega)$, the MEG of an antenna with 100% total efficiency is always $G_{\mathrm{e,Uniform}} = 1/2$. For any other propagation scenarios given by a specific $P_{\theta,\phi}(\Omega)$, such as the Gaussian distribution in (9), G_{e} needs to be evaluated numerically using (10).

However, the MEG metric in (10) is usually evaluated using normalized antenna gain patterns. As discussed in [5], MEG corresponds to the antenna directive gain when the incoming fields are centered at a single direction. In this study, the radiation patterns of the antennas are also normalized. In order to account for the realized antenna gain using the total antenna efficiency η_i that includes mismatch loss, the total gain of the i-th antenna denoted by γ_i in $\mathbf{\Lambda}$ of (6) can be obtained as

$$\gamma_i = \eta_i G_{\mathrm{e},i}, \tag{12}$$

where $G_{\mathrm{e},i}$ denotes the MEG of the i-th antenna port in the given APS.

C. Correlation Coefficient

The complex correlation r between any two antenna elements can be calculated using the complex radiation patterns $E_{\theta,\phi}(\Omega)$ of the antennas, given the propagation scenario $P_{\theta,\phi}(\Omega)$. The correlation coefficient can be calculated as

$$r = \frac{\int \chi E_{\theta,1}(\Omega)E^*_{\theta,2}(\Omega)P_{\theta}(\Omega) + E_{\phi,1}(\Omega)E^*_{\phi,2}(\Omega)P_{\phi}(\Omega)\,\mathrm{d}\Omega}{\sqrt{G_{\mathrm{e},1}}\sqrt{G_{\mathrm{e},2}}}. \tag{13}$$

If we consider two isotropic antennas separated by a distance of d, and given the uniform 3D APS, the correlation coefficient is given by a sinc function. This corresponds to Case A in Fig. 1, where the first zero-crossing point is obtained with $d = \lambda/2$. For non-uniform propagation scenarios, a closed form expression for the correlation coefficient is not always available. Moreover, for realistic antennas and given a specific propagation scenario, the correlation needs to be evaluated numerically using (13). For example, Fig. 1 also evaluates the correlation coefficient of the isotropic antennas under three cases of Gaussian APS with different incident directions and

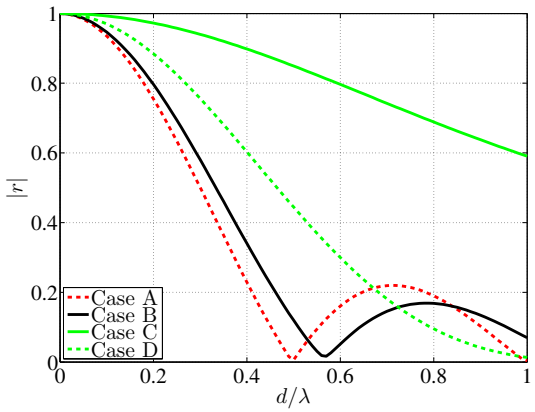

Fig. 1. Correlation of an two-element antenna array in different propagation scenarios as described in Table I.

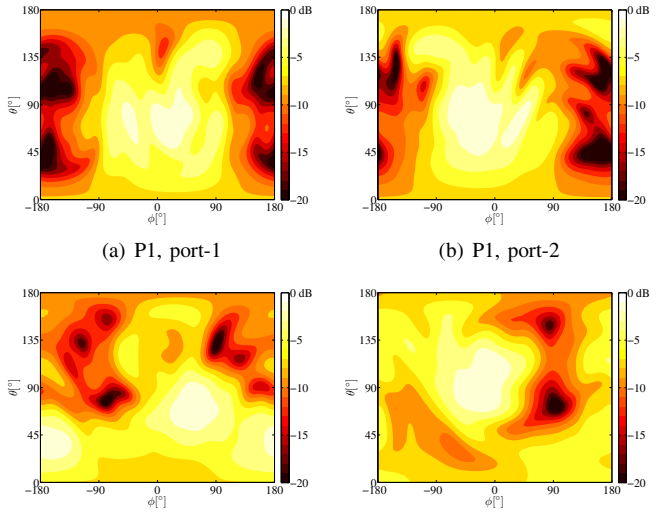

(a) P1, port-1 (b) P1, port-2

(c) P2, port-1 (d) P2, port-2

Fig. 2. Measured radiation patterns $G(\Omega) = G_\theta(\Omega) + G_\phi(\Omega)$ of the two-element antenna prototypes P1 and P2. The patterns are normalized to the maximum gain of each antenna port.

angular spreads (*i.e.*, Cases B-D). Details of the propagation scenarios are provided in Table I. The results show that lower correlation is generally obtained with larger antenna separation and wider angular spread. However, correlation is also determined by the incident direction, which can lead to different interactions between the antennas and the propagation channel. For instance, the end-fire directed scenario (Case C) of the linear array gives a much higher correlation than the more broadside directed scenario (Case D). The reason for the choice of the incident wave directions will be revealed in the following discussion.

III. Evaluation Procedure

One contribution of this paper is to establish a procedure for evaluating the multiplexing efficiency performance of MIMO AUTs in arbitrary propagation scenarios. Using the expression given in (4), the evaluation steps are summarized in the following:

1) Perform simulation or passive measurement of the MIMO AUT and the reference MIMO antennas, in order to obtain $E_{\theta,\phi,i}(\Omega)$ and η_i.
2) Given the propagation scenario with a specific $P_{\theta,\phi}(\Omega)$, calculate $G_{\mathrm{e},i}$ and $\bar{\mathbf{R}}(i,j)$.
3) Form $\mathbf{R}$ and $\mathbf{R}_0$ of (5) using γ_i from (12) and the results obtained from above in 2).
4) Evaluate $\det(\mathbf{R})^{1/M}$ and $\det(\mathbf{R}_0)^{1/M}$.
5) Compute the multiplexing efficiency $\tilde{\eta}_{\mathrm{mux}}$ using (4).

IV. Case Study: 2 × 2 MIMO

To highlight the effectiveness of performance evaluation using the multiplexing efficiency metric, and to investigate the impact of the interactions between the MIMO antennas and the propagation channel, two different two-antenna prototypes are studied. In this case, the correlation matrix $\mathbf{R} = \mathbf{\Lambda}^{1/2}\bar{\mathbf{R}}\mathbf{\Lambda}^{1/2}$ is given by

$$\mathbf{\Lambda} = \begin{bmatrix} \eta_1 G_{\mathrm{e},1} & 0 \\ 0 & \eta_2 G_{\mathrm{e},2} \end{bmatrix}, \bar{\mathbf{R}} = \begin{bmatrix} 1 & r \\ r^* & 1 \end{bmatrix}. \quad (14)$$

The evaluation procedure discussed in Section III requires a reference antenna system. Below, two reference systems are defined using isotropic antennas.

A. Spatial Reference (R1)

In the spatial reference (R1), an array of two isotropic antennas are considered, with a separation distance of $d = \lambda/2$. The isotropic antenna is characterized by $\eta_0 = 1$ and $G_{\mathrm{e},0} = 1/2$. In this case, $\mathbf{\Lambda}_0 = 1/2\mathbf{I}_2$ is obtained in any propagation scenarios. However, the correlation r_0 depends strongly on the APS of the propagation scenario. According to the discussion above, the correlation $r_0 = 0$ is obtained with uniform 3D APS. For Gaussian APSs, (13) needs to be numerically evaluated, with some examples given in Fig. 1.

B. Polarization Reference (R2)

Since polarization diversity is widely used in MIMO antennas, it is important to have a reference system of such kind. In the polarization reference (R2), two ideal cross-polarized antennas are considered, *i.e.*,

$$G_{\theta,1}(\Omega) = G_{\phi,2}(\Omega) = 1, G_{\phi,1}(\Omega) = G_{\theta,2}(\Omega) = 0. \quad (15)$$

R2 ideally gives zero correlation in any propagation scenario.

C. Prototypes

Two realistic two-antenna mobile terminal prototypes (P1 and P2) are evaluated, whose design parameters have been provided in [1]. Since the angular power information is the main focus in studying the impact of the propagation channel, the measured radiation patterns are presented here in Fig. 2. It can be seen that the antenna patterns of P2 exhibit better pattern diversity, whereas the patterns of both antenna elements in P1 share similar radiation characteristics with the main beam direction centered at $(\theta = 90°, \phi = 0°)$. The

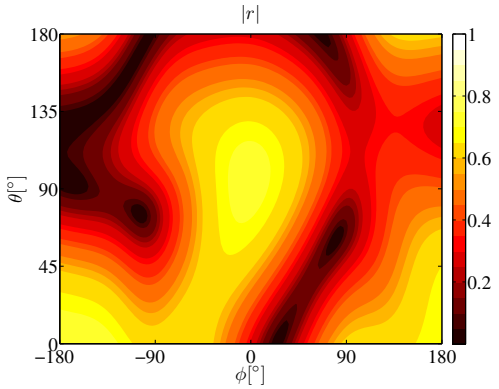

Fig. 3. Correlation pattern of P2 with Gaussian APS at different incident directions with 30° angular spread.

different pattern characteristics lead to the respective MIMO AUTs exhibiting significantly different correlation behaviors. For instance, Fig. 3 illustrates the correlation of P2 with the Gaussian APS at different incident directions with 30° angular spread in both polarizations, *i.e.*, the pattern of correlation coefficient. It shows that higher correlation is obtained at the main incident direction of about $(\theta = 90°, \phi = 0°)$, whereas lower correlation can be obtained at other incident directions, *e.g.*, $(\theta = 60°, \phi = 80°)$. This is due to the better pattern diversity in the antenna patterns of P2 (relative to P1). In contrast, P1 does not provide large variations of the correlation for any incident direction and high correlation is always obtained.

D. Propagation Scenarios

To evaluate the multiplexing efficiency of the two MIMO AUTs P1 and P2, four propagation scenarios with different APSs are considered in Table I. In Case A, the uniform 3D APS is considered as the reference scenario. In other cases, the Gaussian distribution defined in (9) is employed. Case B describes a practically relevant scenario, where the APS concentrates about an elevated angle of $\theta = 30°$, with a spread $\sigma_\theta = 30°$, whereas it is uniformly spread in the azimuth. In Case C, the Gaussian APS is chosen with the incident direction centered at $(\theta_0 = 90°, \phi_0 = 0°)$. Thus, the incident field is

TABLE I
PROPAGATION SCENARIOS.

Case	Distribution
A	Uniform 3D APS
B	Gaussian APS $(\theta_0 = 30°, \phi_0 = 0°)$ $(\sigma_\theta = 30°, \sigma_\phi = \infty)$
C	Gaussian APS $(\theta_0 = 90°, \phi_0 = 0°)$ $(\sigma_\theta = 30°, \sigma_\phi = 30°)$
D	Gaussian APS $(\theta_0 = 60°, \phi_0 = 80°)$ $(\sigma_\theta = 30°, \sigma_\phi = 30°)$

TABLE II
CHARACTERISTICS OF THE REFERENCE AND PROTOTYPE SYSTEMS.

		P1	P2	R1	R2
Port		1, 2	1, 2	1, 2	1, 2
η [dB]		-4.7, -5.2	-3.9, -4.2	0	0
G_e [dB]	A	-3.0, -3.0	-3.0, -3.0	-3.0	-3.0
	B	-2.5, -2.8	-1.4, -3.8		
	C	-0.1, 0.0	-2.1, -0.4		
	D	-1.4, -3.0	-0.2, -6.2		
$\lvert r \rvert$	A	0.80	0.19	0	0
	B	0.87	0.27	0.12	
	C	0.79	0.73	0.85	
	D	0.89	0	0.44	

aligned to the main beam directions of the antenna patterns illustrated in Fig. 2. It is worth noting that this direction also coincides with the end-fire direction of the spatial reference R1. Lastly, Case D considers the case where P2 exhibits low correlation at $(\theta = 60°, \phi = 80°)$ as shown in Fig. 3. It is also approximately the broadside direction of the spatial reference R1.

Throughout the discussion, $\chi = 1$ is assumed without loss of generality. Furthermore, the investigation here is mainly intended to demonstrate the effectiveness of the proposed evaluation approach, rather than to discuss which APS model is more realistic and accurate. Therefore, the four scenarios are chosen to highlight the impact of the interactions between the antennas and the propagation channel. Any other propagation scenarios can be investigated using the same evaluation procedure in a straightforward manner.

E. Numerical Analysis

The total efficiencies, MEGs and correlations of the two MIMO AUTs and the two references in the four propagation scenarios of Cases A-D are summarized in Table II. In this particular example, the expression of $\tilde{\eta}_{\text{mux}}$ can be further simplified as

$$\tilde{\eta}_{\text{mux}} = \sqrt{\frac{4\gamma_1\gamma_2(1-|r|^2)}{1-|r_0|^2}}, \tag{16}$$

where γ_i denotes the total gain of each antenna port of the AUT as defined in (12). We have also used the fact that $G_{e,0} = 1/2$. To re-formulate the above expression in dB scale,

$$\tilde{\eta}_{\text{mux}}\,[\text{dB}] = \tilde{\gamma}\,[\text{dB}] + \tilde{r}\,[\text{dB}], \tag{17}$$

where

$$\tilde{\gamma}\,[\text{dB}] = \bar{\gamma}\,[\text{dB}] - (-3) = \frac{\gamma_1\,[\text{dB}] + \gamma_2\,[\text{dB}]}{2} - (-3) \tag{18}$$

denotes the average antenna gain $\bar{\gamma}$ of the MIMO AUT relative to the reference antenna. Similarly, the correlation-related term is given by

$$\tilde{r} = \sqrt{\frac{1-|r|^2}{1-|r_0|^2}}. \tag{19}$$

TABLE III
EVALUATION OF THE PROTOTYPE ANTENNAS.

		P1				P2			
Case		A	B	C	D	A	B	C	D
$\tilde{\gamma}$ [dB]		-5.0	-4.6	-2.0	-4.1	-4.1	-3.6	-2.3	-4.2
$\tilde{r}$	R1	-2.2	-3.1	0.6	-2.9	-0.1	-0.1	1.1	0.5
[dB]	R2		-3.1	-2.1	-3.3		-0.2	-1.7	0
$\tilde{\eta}_{\mathrm{mux}}$	R1	-7.2	-7.7	-1.3	-7.0	-4.2	-3.8	-1.2	-3.7
[dB]	R2		-7.7	-4.1	-7.5		-3.8	-3.9	-4.2

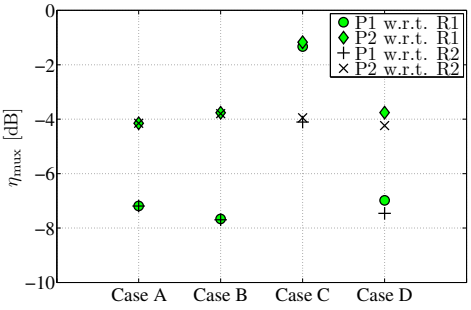

Fig. 4. Summary of the multiplexing efficiency performance of the MIMO AUTs with under different propagation scenarios.

The multiplexing efficiencies of the two MIMO AUTs in the four propagation scenarios, with respect to the two references R1 and R2, are summarized in Table III.

1) Case A: In the uniform case, all antennas are characterized by $G_{\mathrm{e,Uniform}} = -3\,\mathrm{dB}$. For both R1 and R2, $r_0 = 0$ is obtained. The expression (1) can be used directly. According to Table III, the $\tilde{\eta}_{\mathrm{mux,A,2}} = -4.2\,\mathrm{dB}$ of P2 is mainly attributed to practical limitations in antenna efficiency for fully-equipped terminal prototypes (as given in Table II). The low correlation of 0.19 does not have any significant contribution. In comparison, the $\tilde{\eta}_{\mathrm{mux,A,1}} = -7.2\,\mathrm{dB}$ of P1 is due to the $1\,\mathrm{dB}$ lower average antenna efficiency, as well as its high correlation of 0.8, which is responsible for a further $2\,\mathrm{dB}$ loss (see also [1]).

2) Case B: Due to the elevated incident direction, the MEGs of both MIMO AUTs are slightly improved compared to those of the uniform scenario, which can be seen from the higher average antenna gains $\tilde{\gamma}$. However, due to the limited angular spread, higher correlation is also obtained for both MIMO AUTs. In particular, for P1, the loss due to the correlation is $3\,\mathrm{dB}$. As a result, P1 achieves $\tilde{\eta}_{\mathrm{mux,B,1}} = -7.7\,\mathrm{dB}$. The effect on P2 is less significant. Due to the positive contribution from the gain, $\tilde{\eta}_{\mathrm{mux,B,2}} = -3.8\,\mathrm{dB}$ is obtained.

3) Case C: The incident direction of the chosen APS is approximately matched to the main beam direction of the AUTs. In this way, the MEGs of both prototypes are significantly higher than more uniform scenarios such as Cases A&B. The strong MEG partly compensates the lower antenna efficiencies of the AUTs as compared to the reference antennas, *i.e.*, $\tilde{\gamma}$ in Table III. However, the benefit of this power gain comes with a price. The limited angular spread leads to higher antenna correlation. Nevertheless, due to the fact that the APS also coincides with the end-fire direction of the spatial reference R1, its correlation is also as high as $|r_0| = 0.85$. As a result, with respect to R1, very high multiplexing efficiencies of $-1.3\,\mathrm{dB}$ and $-1.2\,\mathrm{dB}$ can be obtained from P1 and P2, respectively. On the other hand, when comparing to the polarization reference R2 that has zero correlation, the multiplexing efficiency is about $2.7\,\mathrm{dB}$ lower for both P1 and P2. This performance loss can be seen from the correlation-related term $\tilde{r}$ in Table III.

4) Case D: This scenario is such that the correlation of P2 is low, as obtained from Fig. 3. In fact, as can be observed in Fig. 2, this is mainly because port 1 of P2 has high gain in the direction $(\theta = 60°, \phi = 80°)$, whereas port 2 has low gain in the same direction. This also leads to large branch power imbalance, which is about $6\,\mathrm{dB}$, as can be seen in Table II. Although the correlation-related contribution is positive in the case of P2 as compared to the reference antennas, the power imbalance is detrimental to the multiplexing efficiency performance. As a result, in Case D, P2 achieves similar multiplexing efficiency as that of the uniform scenario.

V. CONCLUSIONS

In this work, the multiplexing efficiency of MIMO antennas is generalized to consider the impact of the propagation channel. Numerical analysis on some example MIMO antenna prototypes highlights the utility of the metric in quantifying and addressing critical design parameters. For instance, Fig. 4 summarizes the multiplexing efficiency performance of the two prototypes under different propagation scenarios. Except for Case C, P2 that has higher antenna efficiency and better pattern diversity exhibits a more robust multiplexing efficiency performance, with about $3\,\mathrm{dB}$ higher multiplexing efficiency than P1. On the other hand, the low antenna efficiency of P1 is partly compensated by the relatively high MEG in Case C, since the incident direction of the chosen APS in this case is approximately matched to the main beam direction of the MIMO AUTs. This leads to similar multiplexing efficiency of the two prototypes in that scenario.

ACKNOWLEDGMENT

The authors thank Thomas Bolin of Sony Ericsson Mobile Communications AB for his help with the prototypes.

REFERENCES

[1] R. Tian, B. K. Lau, and Z. Ying, "Multiplexing efficiency of MIMO antennas," *IEEE Antennas and Wireless Propag. Lett.*, vol. 10, pp. 183 – 186, 2011.

[2] ——, "Multiplexing efficiency of MIMO antennas with user effects," in *2012 IEEE Int. Symp. Antennas and Propag. (AP-S)*, in press.

[3] F. Athley, A. Derneryd, J. Friden, L. Manholm, and A. Stjernman, "MIMO performance of realistic UE antennas in LTE scenarios at 750 MHz," *IEEE Antennas Wireless Propag. Lett.*, vol. 10, pp. 1337 – 1340, 2011.

[4] R. Vaughan and J. B. Andersen, *Channels, Propagation and Antennas for Mobile Communications*. London: The IEE, 2003.

[5] T. Taga, "Analysis for mean effective gain of mobile antennas in land mobile radio environments," *IEEE Trans. Veh. Technol.*, vol. 39, no. 2, pp. 117 – 131, May 1990.